LA-UR-96-1741

CONF-9605214--1

TITLE: **KEY ISSUES IN PLASMA SOURCE ION IMPLANTATION**

AUTHORS: D. J. REJ, R. J. FAEHL, J. N. MATOSSIAN

RECEIVED
JUN 11 1996
OSTI

SUBMITTED TO: *Surface Coatings and Technologies*

DISCLAIMER

This report was prepared as an account of work sponsored by an agency of the United States Government. Neither the United States Government nor any agency thereof, nor any of their employees, makes any warranty, express or implied, or assumes any legal liability or responsibility for the accuracy, completeness, or usefulness of any information, apparatus, product, or process disclosed, or represents that its use would not infringe privately owned rights. Reference herein to any specific commercial product, process, or service by trade name, trademark, manufacturer, or otherwise does not necessarily constitute or imply its endorsement, recommendation, or favoring by the United States Government or any agency thereof. The views and opinions of authors expressed herein do not necessarily state or reflect those of the United States Government or any agency thereof.

MASTER

Los Alamos
NATIONAL LABORATORY

Los Alamos National Laboratory, an affirmative action/equal opportunity employer, is operated by the University of California for the U.S. Department of Energy under contract W-7405-ENG-36. By acceptance of this article, the publisher recognizes that the U.S. Government retains a nonexclusive, royalty-free license to publish or reproduce the published form of this contribution, or to allow others to do so, for U.S. Government purposes. The Los Alamos National Laboratory requests that the publisher identify this article as work performed under the auspices of the U.S. Department of Energy.

Form No. 836 R5
ST 2629 10/91

DISTRIBUTION OF THIS DOCUMENT IS UNLIMITED

DISCLAIMER

Portions of this document may be illegible in electronic image products. Images are produced from the best available original document.

KEY ISSUES IN PLASMA SOURCE ION IMPLANTATION

D. J. Rej, R. J. Faehl

Los Alamos National Laboratory, MS-D434, Los Alamos, NM 87545, USA

J. N. Matossian

Hughes Research Laboratory, 3011 Malibu Canyon Rd., Malibu CA 90265, USA

ABSTRACT

Plasma source ion implantation (PSII) is a scaleable, non-line-of-sight method for the surface modification of materials. In this paper, we consider three important issues that should be addressed before wide-scale commercialization of PSII: (1) implant conformality; (2) ion sources; and (3) secondary electron emission. To insure uniform implanted dose over complex shapes, the ion sheath thickness must be kept sufficiently small. This criterion places demands on ion sources and pulsed-power supplies. Another limitation to date is the availability of additional ion species beyond B, C, N, and O. Possible solutions are the use of metal arc vaporization sources and plasma discharges in high-vapor-pressure organometallic precursors. Finally, secondary electron emission presents a potential efficiency and x-ray hazard issue since for many metallurgic applications, the emission coefficient can be as large as 20. Techniques to suppress secondary electron emission are discussed.

I. INTRODUCTION

Ion implantation[1] is a well-developed technology used to modify material surface properties, *e.g.*, for manufacturing semiconductor junctions and oxides, and for production of high-strength, light-weight, corrosion-resistant metals. A limitation to more widespread use of implantation for large-area, high-dose applications is the time, expense, and complexity associated with conventional line-of-sight, accelerator-based techniques. Plasma source ion implantation[2-4] (PSII) is a scaleable, non-line-of-sight, batch process that has the potential of overcoming many of these limitations. In PSII a negative high-voltage pulse, typically ranging between 10 and 300 kV and over a period between 1 to 40 μs, is applied to an electrically conducting workpiece immersed in a plasma. The plasma usually consists of a weakly ionized discharge created from a gaseous precursor admitted into a vacuum chamber. Plasma ions are accelerated by the applied electrical potential and are implanted into the surface of the workpiece. Implant times are short when compared to beamline techniques since high-current, pulsed-power supplies compatible with this process can provide nearly two orders of magnitude higher average currents than conventional accelerators. Since large areas can be implanted concurrently, ion current densities to the workpiece can be kept low to avoid overheating problems sometimes encountered in beamline implants. In this paper, we consider three issues which must be addressed before wide-scale commercialization of PSII: (1) implant conformality; (2) ion sources; and (3) secondary electron emission.

II. IMPLANT CONFORMALITY

An attractive feature of PSII is that it is non-line-of-sight. Cumbersome workpiece manipulation fixtures and beam rastering are unnecessary. System efficiencies are high since

the perpendicular trajectories into the workpiece eliminate the need for masking. However, implants conform around complicated shapes as long as the plasma sheath dimensions remain small compared to the workpiece feature sizes. For certain applications, this condition may not be easily attained because of hardware limitations.

The evolution of supersonic ion sheaths has been discussed in detail elsewhere.[4-7] In brief, following application of the pulsed negative voltage V, plasma electrons near the surface of the workpiece are rapidly repelled (in a few ns) to uncover a region of uniform ion density. This region is known as the ion matrix sheath and has a thickness s_o for planar geometries of[5]

$$s_o = \sqrt{\frac{2\varepsilon_o V}{en_o}} \qquad (1)$$

where n_o = the initial plasma density, $\varepsilon_o = 8.9\times10^{-12}$ farad/m is the electric permittivity of free space, and $e = 1.6\times10^{-19}$ coul per unit charge is the elemental charge constant. On a longer time scale (~ μs) ions are accelerated across the sheath by the applied electrical field and are driven into the workpiece surface. As ions are implanted, charge imbalance repels more electrons away from the workpiece, thereby forcing the sheath to expand outward from the workpiece to uncover more ions For planar geometries the sheath thickness s(t) expands at rate[6]

$$s(t) = s_o \sqrt[3]{\frac{2}{3}\omega_{pi}t + 1} \qquad (2)$$

where $\omega_{pi} = [n_o e^2/\varepsilon_o M]^{1/2}$ and M is the ion mass. The pulse length and the ion density are usually adjusted so that the sheath conforms to the workpiece and remains contained inside the vacuum chamber, and so that sheath overlap between adjacent workpieces is avoided. For a

given average power, a smaller sheath is achieved with higher n_o accompanied by higher pulsed currents, and lower repetition rates; moreover, a lower repetition rate allows more time for plasma ions to diffuse back into the depleted sheath region between pulses.[8] However, for a given V, n and s, the ion current is fixed and is given by the Child-Langmuir equation which for planar geometry is

$$j_i(t) = \frac{4\varepsilon_o}{9}\sqrt{\frac{2e}{M}}\frac{V^{3/2}}{[s(t)]^2} \tag{3}$$

The corresponding electrical resistance R_{pl} of the plasma load for an expanding planar sheath is obtained by combining Eq. 3 with Ohm's law,

$$R_{pl} = \frac{9}{4\varepsilon_o}\frac{s^2}{A(\gamma+1)}\sqrt{\frac{M}{2eV}} \tag{4}$$

where A is the workpiece area, and γ is the secondary electron emission coefficient. In PSII the high-voltage pulser must be capable of driving R_{pl} which can be rather small. For example, for a 50 kV N^+ implant with s=10 mm, A= 5 m^2 and γ=7, R_{pl} is 0.76 Ω (corresponding to a total pulsed current of 65 kA). Most pulsers are incapable of driving this load, so users are often forced to compromise by implanting with larger s.

Insight into conformality issues is gained from the computer simulation shown in Fig. 1 and 2 which are from electromagnetic particle-in-cell (PIC) calculations[9] to model the self-consistent evolution of PSII of two automobile pistons.[10-11] The numerical methodology in PIC simulations is that the full set of Maxwell's equations, including displacement currents, is solved at each time step on a regular Eulerian mesh. In these cylindrical (r,z) calculations, the radial and axial resolution is 2 and 1.5 mm, respectively, which is sufficiently smaller than s(t)

which ranges between 16.5 and 105 mm in this series of calculations. The plasma is modeled by an array of 26,000 electrons and 26,000 $C_2H_2^+$ acetylene ions, which are initially cold with a uniform density n_o of either 2.5×10^{14}, 10^{15}, or 10^{16} ions/m^3.

Each workpiece has a gross outer diameter of 82 mm and length of 50 mm. They are electrically connected to an external voltage supply by a cantilevered rod and surrounded by a 318-mm-diam concentric vacuum chamber. In the calculation, the voltage is fed through a 65.8-Ω coaxial line, and has a pulseshape consisting of a 50 ns linear rise followed by a 20 μs flattop. However, calculations are carried out to only 1 μs. For the magnitude of the ion current which is being drawn, the load impedance R_{pl} is much greater than the line feed impedance. The operating point of this circuit is, therefore, essentially twice the source voltage. Calculations are conducted for a bias voltage of 25.3 kV, while secondary electron emission (*cf.* Sec. IV) is neglected.

The calculations yield the self-consistent expanding sheath position s(r,z) as a function of time (Fig. 1) which has both qualitative and quantitative implications. For $n_o=10^{16}$ m^{-3}, we find $s_o=17$ mm which reveals conformality during early times. At 2.5×10^{14} m^{-3}, however, s_o is 105 mm, indicative of poor conformality at all times. For all cases, as the sheath grows, its form changes from an approximately cylindrical to spherical shape, while the ion current decreases consistent with the Child-Langmuir scaling.

Quantitative information extracted from the simulations includes the time-integrated average energy E, implanted dose D_i, and mean angle of incidence θ of implanted ions along the surface of the workpiece as a function of time. The plots in Figure 2 are for t=80, 180, and 480 ns. The time t= 80 ns corresponds to a time shortly after the ion matrix phase has

been established. Relatively few, low-energy ($\leq$ 7 keV) ions have reached the workpiece by this time, especially at low n_o. By t=180 ns, the ion matrix is becoming depleted at the low n_o, but has not yet reached the Child-Langmuir equilibria. Integrated ion energies rise to $\leq$ 14 keV, though this number still includes contributions from the early-time, low-energy ions. By t=480 ns, the ion matrix has been depleted in all cases and Child-Langmuir flow has begun, and E rises to $\leq$ 19.5 keV. This cannot be directly collated to the snapshot of the particle distributions in Fig. 1 since ion transit times are comparable to this time. At t= 980 ns, the instantaneous flux is characterized by energies of 22.7-23.2 keV. E does not reach the full bias voltage because of the finite expansion of the sheath during one transit time.[8] The time elapsed between ion entry into the sheath edge and implantation in the object is of order ω_{pi}^{-1} or about 450-500 ns for the $n_o = 10^{15}$ m^{-3} case. As ions accelerate through the potential well, the well changes both in magnitude and shape. Ion energies are therefore distributed with different energies as one scans along the surface of the object. As the plasma density is increased, so does the dose at any given elapsed time. The increase in dose scales less than linearly with n_o. Also, we find that E at a given time, is slightly greater at higher n_o. Finally, we note that higher n_o leads to more nearly normal ion flow incidence. At later times, this difference begins to relax. This situation is roughly what we expect, based upon the higher degree of conformality which is seen when comparing higher to lower density calculations. Much later in time, as all sheaths lose conformality, we expect this difference to be diminished.

D_i varies by almost 25% along the surfaces. This is due to what might be termed "spherical convergence." Although the exact details depend on the geometry of the implanted object, much of this effect results from intersecting a spherically converging flow with a

cylindrical object. While it does not account for the exact dose pattern, it is useful and generic in understanding dose distributions in long cylindrical arrays of objects. It should be noted, however, that the high density "spikes" at corners of the workpieces are mostly numerical artifact. At a corner, the numerical diagnostic "counts" all ions entering a cell, not just those crossing the outer surface. The retained dose D_r is a more relevant parameter for characterizing implantation than total absorbed dose. D_r depends upon both E and θ. $\theta(z)$ profiles are plotted in Fig 2. The profile and retained dose is estimated with the *Profile Code*[12] for $D_i = 2\times10^{17}cm^{-2}$, E=12 keV implants of C into Al. From the results in Fig. 3, shallower profiles and lower D_r are observed as θ increases, because of the geometric spreading of the incident ion flux and increased sputtering.

A final point about the electron and ion distributions in Fig. 1 should be noted. Large "holes" can be seen at the axial end-faces at later times. These evacuated regions reflect that all of the initial plasma in our numerical chamber has been exhausted. In a physical chamber with the same dimensions, the same phenomenon will occur. Increasing the axial length of the chamber will delay the onset of plasma exhaustion. Simple estimates indicate that a sufficiently long voltage pulse can lead to complete plasma usage in even large PSII chambers. Addressing this issue quantitatively, however, requires considerations of the strength of the plasma source and the bias voltage, which are beyond the scope of the present paper. The process of plasma exhaustion in small chambers can be a real effect and should be evaluated when designing a PSII process.

III. PLASMA SOURCES

PSII requires the generation of a plasma with sufficient density n_o and uniformity around complex-shaped workpieces. As discussed in Sec. II, the value of n_o depends on the required sheath thickness s and implant voltage V, while s depends on several job-specific factors such as workpiece geometry, area, feature size, the process time, and the high-voltage pulser characteristics. Ion species composition is another factor that influences the choice of a plasma sources. With molecular gases, one often creates multiple species, *e.g.*, N_2^+ and N^+ with a N_2 fill; consequently, heavier molecules are accelerated to lower velocities and are implanted into shallower depths than lighter ones. For many metallurgical applications, a mixture of ion species is tolerable (and even desirable) to distribute ions more uniformly into the workpiece surface layer. In general, however, one usually prefers to fully dissociate molecular ions to maximize ion velocity, thereby maximizing implant depth and minimizing sputter losses.

Typical experiments are operated with n_o between 10^{14} and 10^{18} ions/m^3, created in a gas fill density between 10^{19} and 3×10^{20} atoms/m^3 (0.3 to 10 mTorr). Plasma sources utilizing biased filaments and radio frequency electric fields are routinely used. To date, a limitation to more wide-spread use of PSII technology is the availability of additional ion species beyond B, C, N, and O. Two possible solutions are the use of filtered metal arc vaporization sources[13-15] and the use of plasma discharges in high-vapor-pressure organometallic precursors.[16] The principal advantage of the metal arc is atomic control of the ions produced and the ability to create multiply-ionized charge states. Vacuum arc sources have been developed for a wide range of metals and are used in beamline implants. Their use in PSII systems is more suited to higher doses ($>10^{17}$ cm^{-2}) and lower energies (tens of keV) than the usual ranges in

conventional metal ion implantation.[15] The advantage of organometallic precursors is their high volatility, which translates into high fill pressures and high plasma densities, which in turn allow for high ion currents and implantation rates. While several precursors currently exist, their use in PSII systems remains to be validated.

IV. SECONDARY ELECTRON EMISSION

Secondary electron emission is another important feature of PSII. As each ion is implanted, electrons are liberated from the workpiece and are rapidly accelerated through the sheath potential. The energetic secondaries stream along essentially collisionless trajectories until they strike and are stopped by grounded objects such as the vacuum chamber walls. For many of the envisioned metallurgic applications, the secondary emission yield γ is large, often ranging between 5 and 20.[17] Therefore, uncontrolled secondary emission could reduce PSII system efficiencies to as low as 5%. Furthermore, the bremsstrahlung x-rays produced by energetic electron bombardment of the chamber walls pose a potential safety hazard.

Lead-shielding is a conventional technique used to provide x-ray shielding in PSII facilities. For implantation voltage up to 100 kV, and total average secondary electron currents of 1 A, lead thicknesses of 7 mm surrounding a vacuum chamber vessel is sufficient to maintain low x-ray flux levels that usually will comply with safety regulations. For many applications, however, implantation voltages well in excess of 100 kV are desirable. For these voltage ranges, the use of lead shielding becomes impractical, since as the implantation voltage is increased from 100 to 300 kV, the x-ray absorption cross section for lead drops by approximately a factor of 20. The lead shielding thickness increase required to accommodate this reduction in absorption becomes

impractical. Therefore, there is a need for methods to reduce or minimize x-ray production in a PSII system.

A technique used to suppress secondary x-ray generation and possibly increase system efficiency, is illustrated in Fig. 4.[18] The technique is based on electrostatic confinement of the secondary electrons. Secondaries are trapped within a metal enclosure supported from the vacuum chamber walls, which is biased to the same electrical potential as the workpiece. A remote plasma source produces a plasma near ground potential. A plasma sheath forms around the part, as well as along the entire surface of the enclosure. When voltage is applied to the workpiece, it also is applied to the entire enclosure. The applied voltage develops across the sheath between the plasma and the workpiece, and also between the plasma and the enclosure. Therefore, ions are implanted into both the workpiece and the enclosure. Secondary electrons emitted from the workpiece and the enclosure are repeatedly reflected within the interior of the enclosure, and they are prevented from impacting the grounded vacuum chamber walls. The only grounded surface available for x-ray production is the plasma source, whose area can be minimized. The secondary electrons may dissipate their energy into the plasma during reflections from the enclosure walls, possibly aiding in the production of additional plasma. This could increase the efficiency of the PSII system by transferring secondary-electron energy into the plasma production process.

Recent experiments using this technique at the Hughes Research Laboratory at 50 kV voltage levels have reduced the unshielded x-ray level from 20 mrad/hour to a level below the minimum detection limit (< 0.2 mrad/hour). At 80 -kV operation, the unshielded x-ray level is reduced by a factor of four. Experiments were conducted with an enclosure constructed from the

same material as the workpiece to ensure that the secondary electron yield for all surfaces was the same. PSII was conducted with N_2^+ ions with and without the enclosure in place, ensuring that the total average current from the high-voltage pulser was maintained constant. This ensured that the total incident ion current to all the interior surfaces of the enclosure was the same. X-ray dosimeter readings at an unshielded glass window located at the front of the vacuum chamber are shown in Table I. Uniform D_r of $1\times10^{17}cm^{-2}$ have been confirmed with secondary ion mass spectroscopy on implanted 6×6 mm stainless steel coupons affixed at various locations to the workpiece and enclosure walls during the PSII experiments.

There exist other proposed (but unproven) techniques for suppressing secondary electrons. One method involves using negative ions and positive accelerating voltages. Negative ion sources have been developed for high-energy particle accelerators. The extrapolation of these sources to supply the large average currents demanded by PSII remains a challenge; furthermore, maintaining a high negative ion to electron density ratio will be essential to minimize unwanted primary electron currents and x-ray emission. A second method uses multiply-charged ions which will reduce the required acceleration voltage, bremsstrahlung generation, and shielding requirements. Indeed vacuum arc sources are well known for their ability to produce multiply-charged species.[14] However, with multiply-charged ions come increased secondary electron yields which must also be contended with and accounted for. A third method uses an externally applied magnetic field.[19] Secondary electrons are trapped in the field to form a virtual cathode layer near the workpiece surface where the local electric field is substantially reduced. Subsequent electrons that are emitted can then be reabsorbed by the workpiece. The magnitude of B is chosen so that secondary electron trajectories are greatly

altered, while ion motion is only slightly perturbed. With this technique, care must be taken in using it in conjunction with magnetic workpieces (such as steel components or dies) which can alter the magnetic field being used for secondary-electron trapping, or may itself become permanently magnetized during the process.

V. CONCLUSION

The appeal of PSII is that it enables one to apply the well-known benefits of ion implantation in a quick and cost-effective manner to complex shapes. However, to take full advantage of the non-line-of-sight property of PSII, it is important to maintain sufficiently small sheath thickness to insure a uniform implant. In some cases, this can not be easily accomplished because pulsed power supplies are incapable of driving the relative low load impedance that results from small sheaths. As a compromise, additional fixturing or multiple workpiece configurations should be implemented to eliminate edge field phenomenon that affect implant uniformity. Another limitation at the present time is the availability of additional ion species beyond B, C, N, and O. Both vacuum arc and volatile organometallic ion sources have been developed to enable PSII with metallic ions. Finally, substantial secondary electron emission often accompanies PSII, limiting electrical system efficiencies. While the suppression of secondaries remains an ongoing part of current research, virtually all PSII devices are operated without any secondary electron control. Consequently, adequate x-ray shielding is an important part of any PSII machine. It should be noted, however, that cost projections[20] for commercial PSII indicate that the poor efficiencies caused by secondary electron losses do not dramatically alter the overall expenses since the additional capital and utility costs for the high-voltage pulser system are a relatively minor part of the total expense.

ACKNOWLEDGMENTS

PSII research at Los Alamos National Laboratory is supported by the U.S. Department of Energy Defense Programs Technology Transfer Initiative, and through the U.S. Dept. of Commerce Advanced Technology Program. The Hughes Research Laboratory portion of this paper has been supported by Hughes Internal Research and Development Funds.

REFERENCES

[1] Nastasi M and Meyer J W 1996 *Ion Solid Interactions: Fundamentals and Applications* (Cambridge Univ. Press, 1996)

[2] Conrad J R, Radtke J L, Dodd R A, Worzala F J and Tran N C 1987 *J. Applied Physics* **62** 4591-6

[3] Conrad J R 1988 *U. S. Patent 4,764,394*

[4] Rej D J, in *Handbook of Thin Film Technology,* edited by D. Glocker and I. Shah (supplement 1, Inst. of Physics Publishing, in press).

[5] Andrews J G and Varey R H 1971 *Phys. Fluids* **14** 339-43

[6] Scheuer J T, Shamim M and Conrad J R 1990 *J. Appl. Physics* **67** 1241-5

[7] Kissick M W, Hong M P, Shamim M M, Callen J D 1994 *J. Appl. Phys.* **76** 7616-18.

[8] Wood B P 1993 *J. Appl. Phys.* **73** 4770-8

[9] Faehl R J, DeVolder B and Wood B 1994 *J. Vac. Sci. Technol.* **B12** 884-8

[10] Nastasi M, Elmoursi A A, Faehl R J, Hamdi A H, Henins I, Malaczynski G W, Mantese J V, Munson C P, Qui X, Reass W A, *et al.,* 1996 *Proc. Mat. Res. Soc.* (in press)

[11] Malaczynski G W, Qiu X, Mantese J V, Elmoursi A A, Hamdi A H, Wood B P, Walter K C and Nastasi M A 1995 *U.S. Patent 5,458,927*

[12] The *Profile Code™* is available from Implant Sciences Corp., Wakefield, MA 01880.

[13] Adler R J and Picraux T 1985 *Nucl. Instrum. Methods Phys.* **B6** 123-8

[14] Brown I G and Washburn J 1987 *Nucl. Instrum. Methods Phys.* **B21** 201-4

[15] Brown I G, Anders A, Anders S, Dickenson M R and MacGill R A 1994 *J. Vac. Sci. and Technol.* **B12** 823-827

[16] Healy M D and Smith D C 1993 *Materials Technology* **8**, 149-52

[17] Shamim M M, Scheuer J T, Fetherston R P and J. R. Conrad J R 1991 *J. Appl. Phys.* **70** 4756-9

[18] Matossian J N 1996 U.S. Patent (pending)

[19] Rej D J, Wood B P, Faehl R J and Fleischmann H H 1994 *J. Vac. Sci. Technol.* **B12** 861-6

[20] Rej D J; Alexander R B 1994, *J. Vac. Sci. Technol.* **B12** 2380-2387.

Table I. Effect of electrostatiuc confinement on PSII x-ray emission

V (kV)	Total current to plasma (mA)	Enclosure used?	Dosimeter reading (mRad/hr)
50	20	No	20
50	20	Yes	<< 1
75	15	No	85
75	15	Yes	20

FIGURE CAPTIONS

Fig. 1 Particle-in-cell simulations of PSII into two automotive pistons for initial plasma $C_2H_2^+$ densities n_o of (a) 2.5×10^{14}, (b) 10^{15}, and (c) 10^{16} ions/m^3. Positions of electrons (red) and ions (blue) are plotted for times t= 80, 180, and 480 ns into the PSII pulse.

Fig. 2 Time-integrated average energy E, implanted dose D_i, and mean angle of incidence θ of implanted ions along the outer surface of the pistons for initial plasma $C_2H_2^+$ densities n_o of (a) 2.5×10^{14}, (b) 10^{15}, and (c) 10^{16} ions/m^3 at times t= 80, 180, and 480 ns.

Fig. 3 (a) Computed profiles for a $D_i = 2\times10^{17}$ cm^{-2} implant of 12 keV carbon into aluminum with angle of incidence θ = 0, 20, 40, and 60°. (b) Retained dose D_r as a function of θ.

Fig. 4 Control of secondary electrons by a biased enclosure.

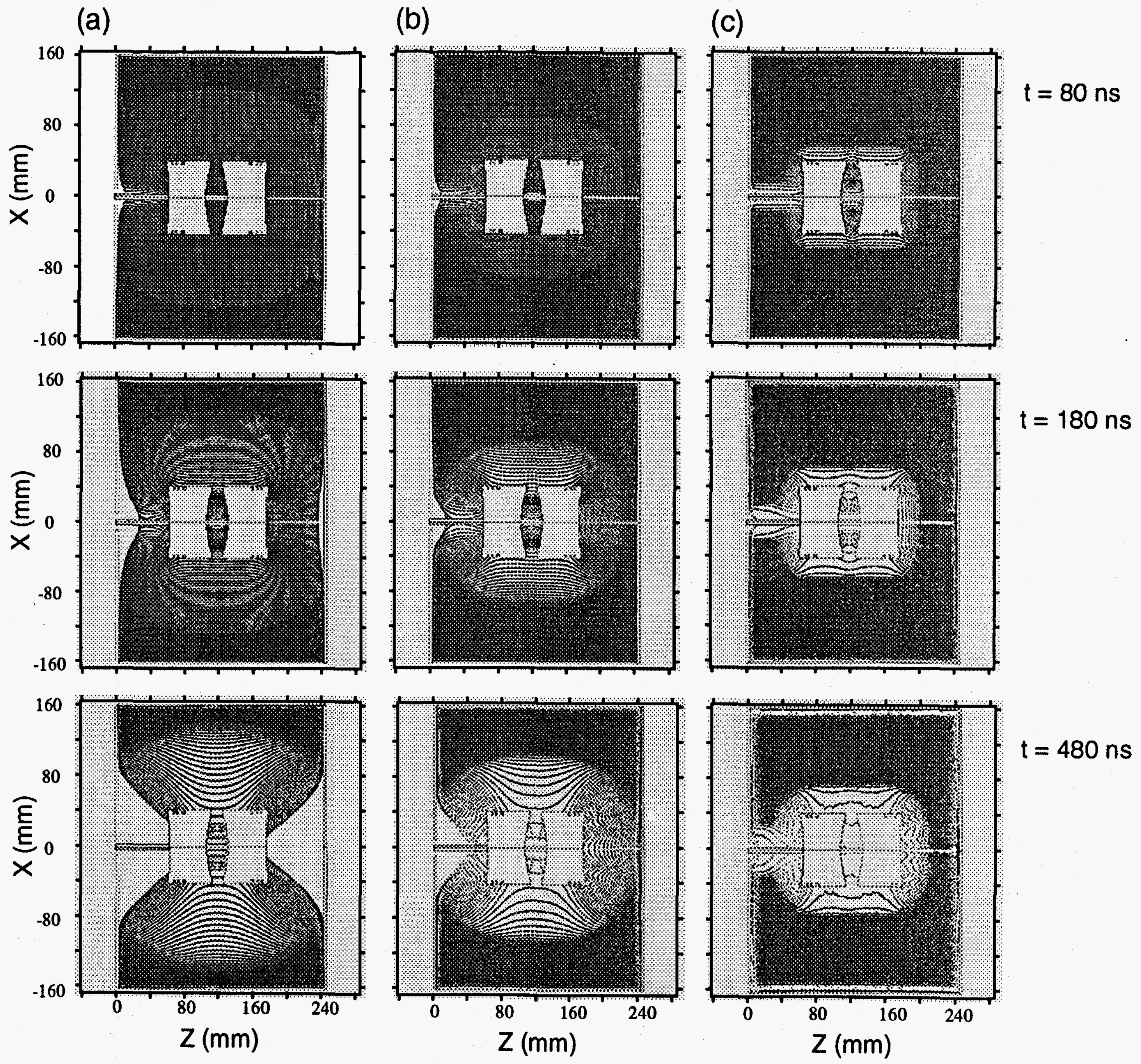

Fig. 1

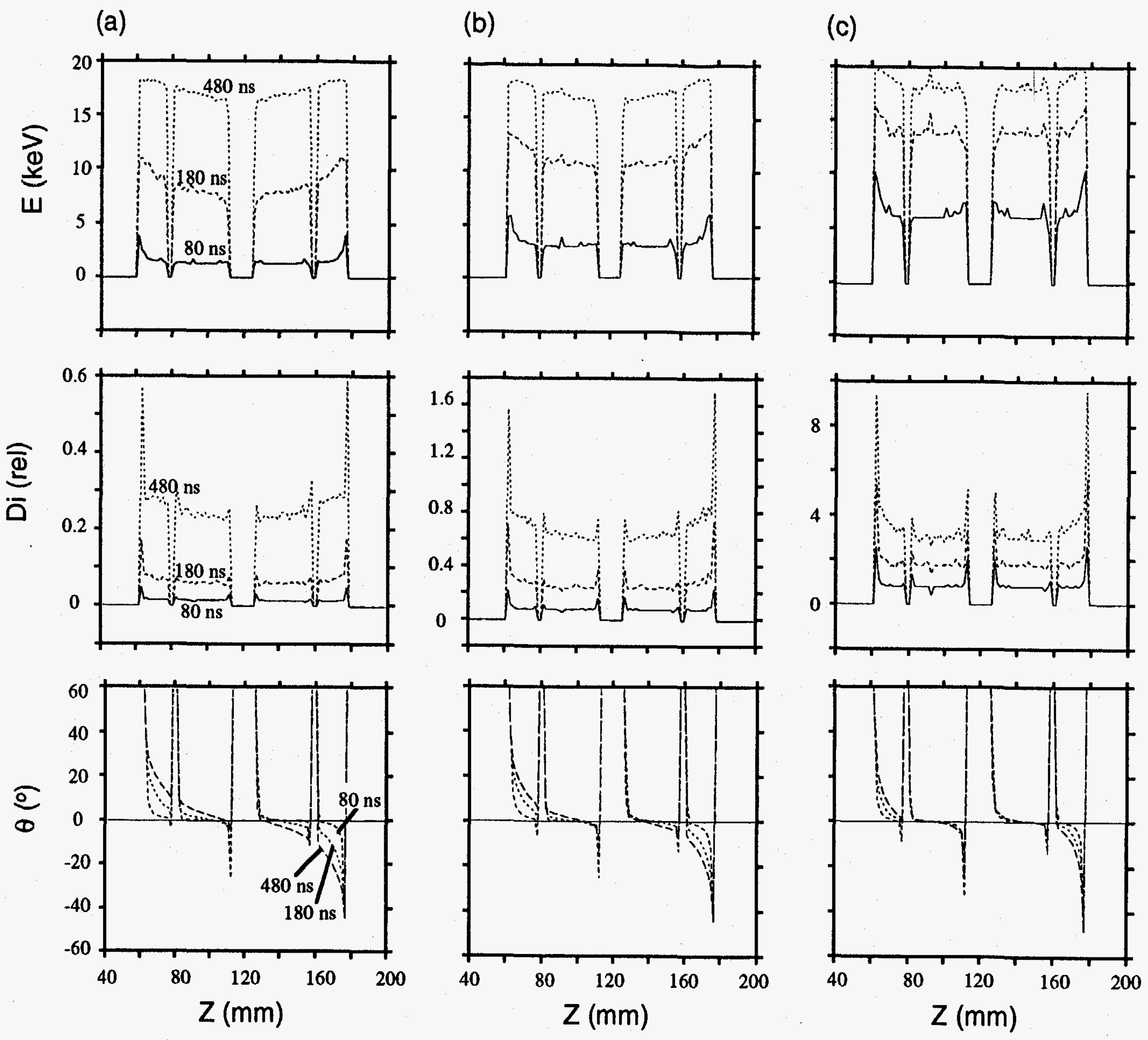

Fig. 2

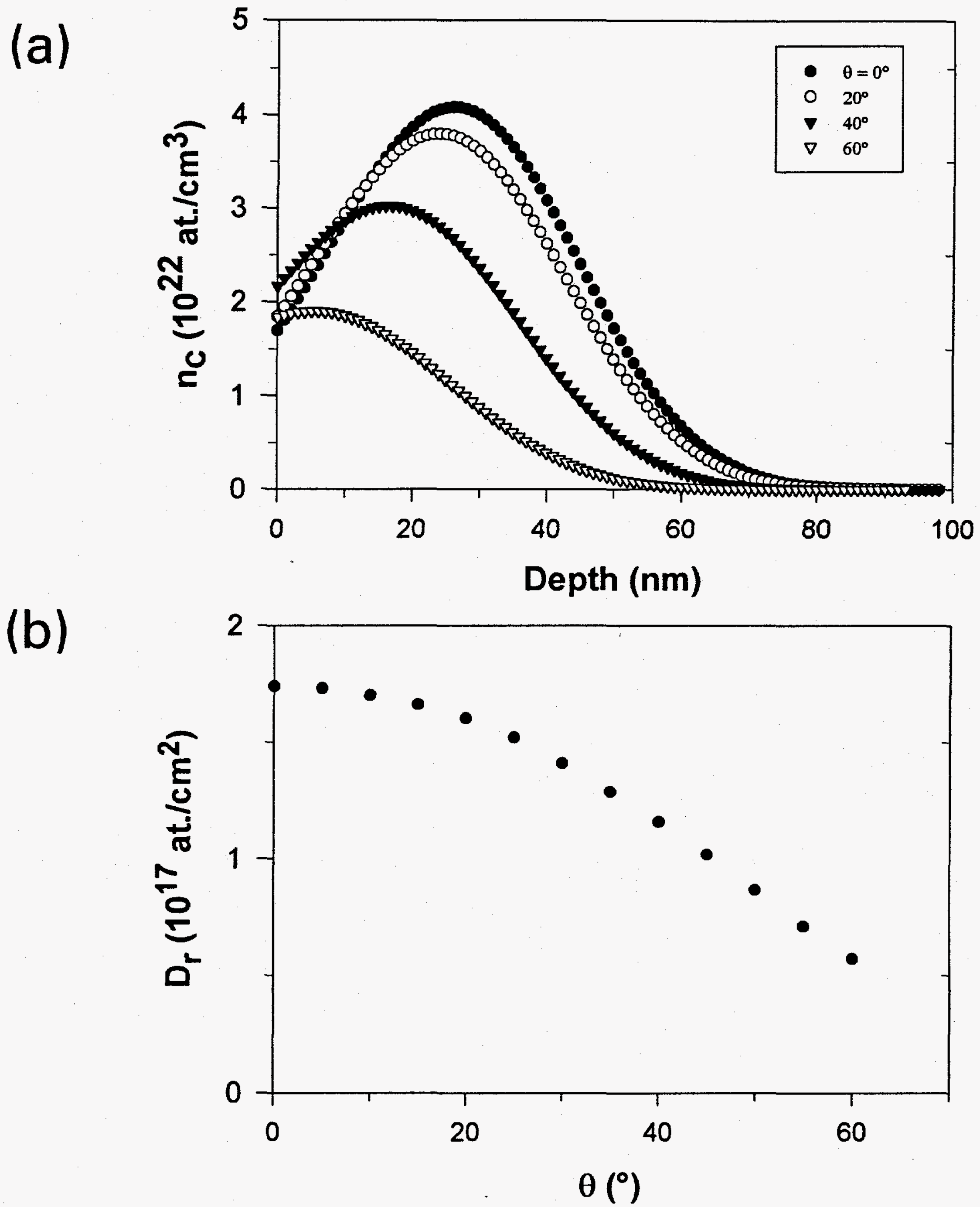

Figure 3

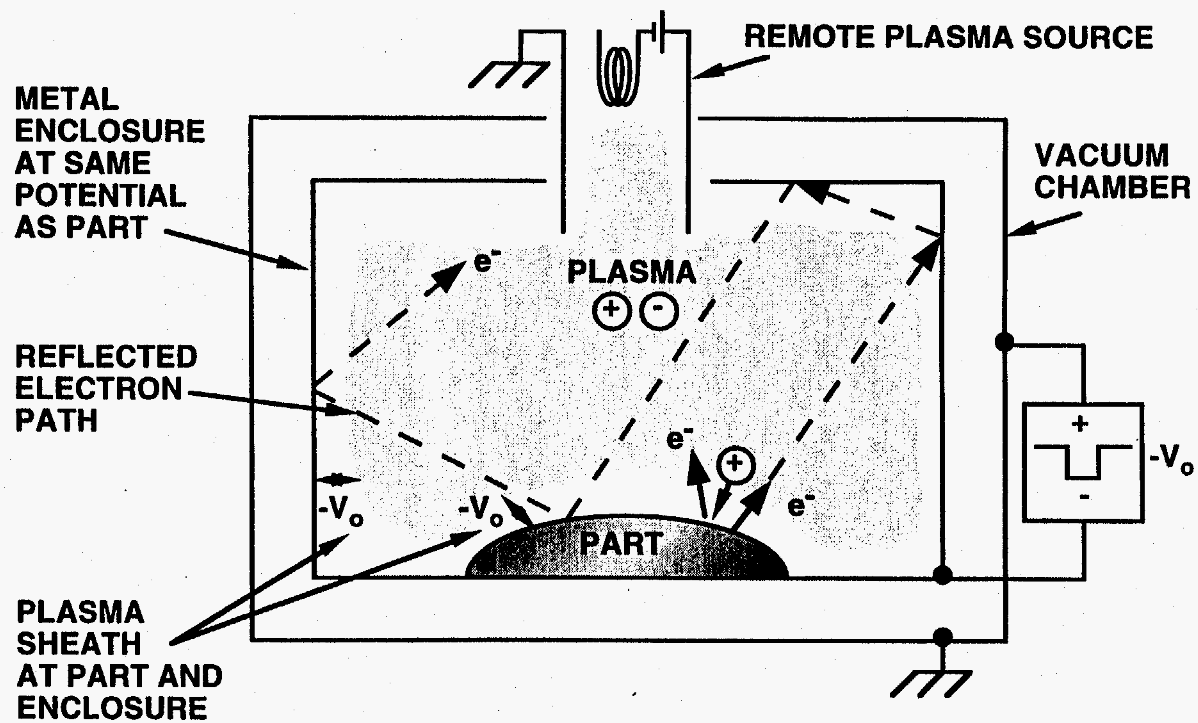

Fig. 4